1. Mohamed Essalih BOUSSOUAR[1], 2. Khaled YAHIA[1], 3. A.J.M CARDOSO[2], 4. Mohamed SAHRAOUI[1]

University of Mohamed Khaidar, Biskra, Algeria (1), University of Beira Interior, Covilhã, Portugal (2)

Enhanced Direct Torque Control of a Syn-RM, Using Adaptive Flux Observer, Including Magnetic Saturation and Iron Losses

Abstract. An enhanced direct torque control (E-DTC) system of a synchronous reluctance motor (Syn-RM) is presented in this paper. The motor system is modelled by taking into account its non-linear behaviours such as iron losses and magnetic saturation. The proposed method consists of incorporating hysteresis DTC with a model reference adaptive system (MRAS) flux observer. This technique is applied in order to achieve good torque and flux ripples reduction, which ensure a smooth operation of the Syn-RM along all the speed range. Furthermore, the proposed method has simple design and implementation in the overall control system, and can avoid the drawbacks of conventional flux estimators. Simulation results show the effectiveness of the proposed method.

*Streszczenie. W artykule przedstawiono udoskonalony układ bezpośredniego sterowania momentem obrotowym (E-DTC) synchronicznego silnika reluktancyjnego (Syn-RM). Układ ruchu jest modelowany z uwzględnieniem jego nieliniowych zachowań, takich jak straty żelaza i nasycenie magnetyczne. Proponowana metoda polega na włączeniu histerezy DTC do wzorcowego obserwatora strumienia adaptacyjnego systemu odniesienia (MRAS). Technika ta jest stosowana w celu uzyskania dobrego momentu obrotowego i redukcji tętnień strumienia, które zapewniają płynną pracę Syn-RM w całym zakresie prędkości. Ponadto, zaproponowany sposób ma prostą konstrukcję i implementację w całym systemie sterowania i pozwala uniknąć wad konwencjonalnych estymatorów strumienia. Wyniki symulacji pokazują skuteczność proponowanej metody..(**Ulepszona bezpośrednia kontrola momentu obrotowego Syn-RM, wykorzystująca adaptacyjnego obserwatora strumienia, w tym nasycenie magnetyczne i straty żelaza**)*

Keywords: Direct torque control (DTC), Flux estimation, Torque Ripple
Słowa kluczowe: Bezpośrednia kontrola momentu obrotowego , szacowanie strumienia, tętnienie momentu obrotowego

1. Introduction

In recent years, the synchronous reluctance motor (Syn-RM) has attracted the attention of many researchers all over the world. Syn-RM is considered as a very promising motor for future applications because of its high-power density, superior reliability, due to its simple rotor structure, and outstanding efficiency, especially in torque control applications.

Accurate representation of Syn-RM requires detailed knowledge of the magnetic behaviour in both d and q axes along with cross-saturation at different operating conditions. The iron loss is introduced in the Syn-RM model by adding a shunt resistor in both d and q equivalent circuits. The magnetic saturation is introduced in the motor model using experimentally obtained inductance values in both d and q axes [1].

With the evolution of power electronics and drive systems, the control of such motor has become a big challenge. Advanced field-oriented control has been employed in Syn-RM [2, 3]. Maximum Torque Per Ampere (MTPA) and Flux Weakening (FW) operation modes for Syn-RM have been also proposed [4, 5]. Similar research is dedicated to PM assisted Syn-RM, using estimated load torque [6]. This technique may involve high computational capacity requirements for digital signal processing. In another approach, vector control is applied on PM-assisted Syn-RM parameter uncertain model, by incorporating backstepping current controller [7]. Despite the focus of many researches on the vector control of the synchronous reluctance drive, such motor sufferers from high torque and flux ripples in steady state operation [8, 9]. Direct Torque Control (DTC) is known as one of the most conventional control strategies used for the induction motor (IM) and permanent magnet synchronous motor (PMSM) [10, 11], but rarely used for Syn-RM because of unsatisfying torque and flux response when used in its classic form. An improved duty cycle control method to minimize torque and flux ripples of conventional DTC on IM was then proposed [12].

As it is known, DTC requires instantaneous quantities of the torque and flux that are compared to their reference values within the DTC loop. An improved DTC strategy for a five-phase Interior Permanent Magnet Synchronous Motor

(IPMSM) based on a fuzzy controller is also presented in the literature [13]. This control features a simplicity of implementation, but it suffers from sensitivity to parameters variation, such as stator resistance and/or iron losses. Minimization of the torque ripple in induction and permanent magnet synchronous motors have been widely studied, but few investigations have been conducted on Syn-RM. In this regard, feedback linearization was combined with neuron-fuzzy control for IM torque ripple reduction [14]. Predictive control can be a good alternative for PMSM torque control, and a new Predictive Torque Control (PTC) was proposed to determine the optimal voltage switching states, which ensures less torque and flux ripples [15]. Similar research has been dedicated to PMSM where adaptive learning control was incorporated with an adaptive proportional controller (PI)[16]. The major cons of the later strategy is the important computational capacity requirement and implementation complexity. Optimal current calculation is used, including inductance harmonics [17, 18]. By optimization of the motor design, a combination of asymmetrical poles and shifted pole pairs of Syn-RM has been proposed [19] to have less torque ripple compared to the conventional design. Also, an asymmetrical stator is designed for a ferrite-assisted Syn-RM by shifting the slot opening from the center [20]. The optimization of the flux barrier geometry through the Syn-RM rotor is one of the design solutions for torque ripple reduction where asymmetrical barriers were proposed [21]. A current third-harmonic injection-based technique was also proposed [22], but m = 3 phase number machines are excluded from this research, because the torque produced from the current third-harmonic has a zero-average value. In order to have a fast response of Syn-RM operation, the optimal point of flux reference using MTPA has been investigated [23].
DTC-SVM is employed to achieve extended operation conditions from the point of view of torque and speed, and new MTPA and FW control laws were proposed, but torque ripple reduction was not included [24]. In order to compensate the torque harmonics, an optimal current reference is calculated based on the torque function [25]. This later technique offers simple implementation and less computational complexity.

Most of Syn-RM direct torque control studies have been performed using the flux and torque estimators in their conventional form [13], [23-27]. In this paper an improved DTC with MRAS flux observer is proposed to guarantee a stable operation and less torque ripple against magnetic parameters variation, where smooth operation is achieved at high speeds thanks to back electromagnetic force (EMF) compensation within the flux and torque computation. Moreover, another method of flux angle extraction is proposed. Instead of using voltage-based calculation, the rotor angle position is utilized, shifted by inductance related angle. The effectiveness of the enhanced DTC proposed in this paper is proven by simulation upon a fully nonlinear Syn-RM model.

2. Dynamic Model of the Syn-RM
Syn-RM working principle is based on the anisotropy of reluctance across the rotor, while the stator is similar to other conventional machines. The rotor design generates a direct and quadrature rotating axis, and the corresponding inductances are *Ld* and *Lq*, respectively. The ratio of *Ld/Lq* inductances is straight relative to rotor saliency, which has an effect on the power factor of the motor. Fig.1 illustrates the vector diagram of Syn-RM rotor frame *d,q* shifted by the angle θ_r of the fixed frame axes *α,β* . The Syn-RM measured quantities are expressed in the rotor reference frame d, q, in order to facilitates the control computation and dynamics.

All the quantities expressed in *d,q* reference frame are calculated from stator measurements as [8]:

(i)
$$\begin{cases} i_{d,q} = M_p \; i_{a,b,c} \\ v_{d,q} = M_p \; v_{a,b,c} \end{cases}$$

where *Mp* is the Park transformation matrix, defined as,

(ii)
$$M_p = \sqrt{\frac{2}{3}} \begin{pmatrix} \cos\theta_e & \cos(\theta_e - \frac{2\pi}{3}) & \cos(\theta_e - \frac{4\pi}{3}) \\ -\sin\theta_e & -\sin(\theta_e - \frac{2\pi}{3}) & -\sin(\theta_e - \frac{4\pi}{3}) \end{pmatrix}$$

The presented model of the Syn-RM takes into account iron losses and magnetic saturation. The electrical dynamics are expressed according to the rotor reference frame d,q axes:

(1) $V_d = i_d R_s - w_e L_q i_{qm} + L_d di_{dm}/dt$

(2) $V_q = i_q R_s + w_e L_d i_{dm} + L_q di_{qm}/dt$

where $V_{d,q}$ denotes the direct and quadrature voltages , *Rs* is the stator winding resistor , $L_{d,q}$ and $i_{d,q}$ are the direct and quadrature inductances and currents, respectively , $I_{dm,qm}$ are the currents producing torque, and w_e is the electrical angular speed. The relation between stator currents i_d, i_q and torque producing currents i_{dm}, i_{qm} are stated as follows:

(3) $i_d = i_{dm} - \frac{1}{R_c}\left(w_e L_q i_{qm}\right)$

(4) $i_q = i_{qm} - \frac{1}{R_c}\left(w_e L_d i_{dm}\right)$

As described in Equations (3), and (4) iron losses are presented as an additional resistor *Rc*.
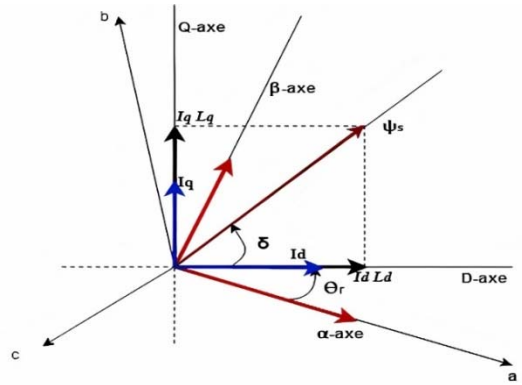

Fig.1. Vector diagram of Syn-RM and coordinate axes.

3. Proposed Direct Torque Control (E-DTC)
3.1. Conventional DTC
As it is shown in Fig.2, this technique consists of controlling torque and flux separately. Speed PI controller generates the electromagnetic torque reference T_{eref} which is compared with the estimated value $\hat{T}_e$, as well as the flux control. The reference value ψ_{ref} is compared with the estimated flux $\widehat{\psi_s}$, and two hysteresis comparators are used for errors judgment, generating three command law possibilities for torque and two for flux.
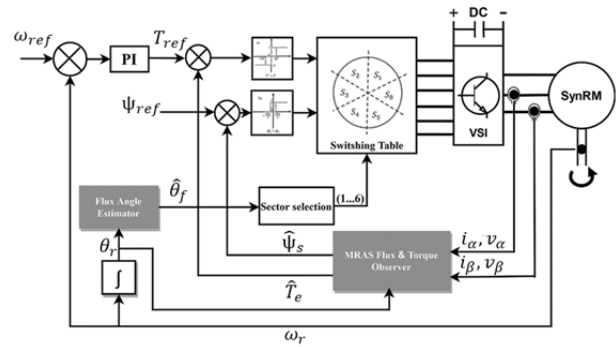

Fig.2. Overall, Syn-RM control scheme of the proposed DTC.

(iii)
$$\begin{cases} T_e^* = 1 \;, \;\; for \;\; \varepsilon_{Te} \rangle H_{Te} \\ T_e^* = 0 \;, \;\; for \;\; H_{Te} \rangle \varepsilon_{Te} \rangle - H_{Te} \\ T_e^* = -1 \;, \;\; for \;\; \varepsilon_{Te} \langle -H_{Te} \\ \psi_s^* = 1 \;, \;\; for \;\; \varepsilon_{\psi s} \rangle H_{\psi s} \\ \psi_s^* = -1 \;, \;\; for \;\; \varepsilon_{\psi s} \langle -H_{\psi s} \end{cases}$$

where T_e^*, ψ_s^* denote torque and flux commands, ε_{Te} , $\varepsilon_{\psi s}$ denote the errors, and H_{Te} , $H_{\psi s}$ are hysteresis pre-set bandwidths. According to Table 1 the plane of the voltage vectors is divided into six sectors. Then, an optimal switching strategy is defined for each sector. The purpose of direct torque control is to restrict the torque error and the stator flux error within a pre-set hysteresis bandwidth. An optimal switching pattern is selected to generate the required torque and flux of the motor. Hence, a closed-loop torque control is obtained.

Table 1. DTC switching table

Sectors		1	2	3	4	5	6
Flux	Torque						
$\psi_s^* = 1$	$T_e^*=1$	V2 (110)	V3 (100)	V4 (101)	V5 (001)	V6 (011)	V1 (010)
	$T_e^*=0$	V7 (111)	V0 (000)	V7 (111)	V0 (000)	V7 (111)	V0 (000)
	$T_e^*=-1$	V6 (011)	V1 (010)	V2 (110)	V3 (100)	V4 (101)	V5 (001)
$\psi_s^* = -1$	$T_e^*=1$	V3 (100)	V4 (101)	V5 (001)	V6 (011)	V6 (010)	V2 (110)
	$T_e^*=0$	V0 (000)	V7 (111)	V0 (000)	V7 (111)	V0 (000)	V7 (111)
	$T_e^*=-1$	V5 (001)	V6 (011)	V1 (010)	V2 (110)	V3 (100)	V4 (101)

3.2. Syn-RM Flux Model

The conventional flux estimation is based on voltage and current quantities in the stator reference frame α; β and can be expressed as:

$$(5) \qquad \Psi_\alpha = \int (V_\alpha - i_\alpha R_s) dt$$

$$(6) \qquad \Psi_\beta = \int (V_\beta - i_\beta R_s) dt$$

The flux angle can be extracted from Equations (5) and (6) as:

$$(7) \qquad \theta_s = \arctan \frac{\Psi_\beta}{\Psi_\alpha}$$

The flux estimator expressions are [28]:

$$(8) \qquad \psi_d = L_d i_d$$

$$(9) \qquad \psi_q = L_q i_q$$

where $\psi_{d,q}$ are flux quantities in the rotor reference frame.

As it is well known, voltage-based flux estimator in Equations (5), and (6) has a negative effect on the DTC quality due to poor filters settings and/or the voltage offset effect, as well as inductances-based flux estimator described in Equations (7), and (8). The proposed method for optimal flux observer is based on the dynamic model in the rotor reference frame *d,q* of the Syn-RM, and it is expressed as:

$$(10) \qquad \widehat{\psi_d} = \int \left(V_d - \hat{i_d} R_s + \widehat{\psi_q} \widehat{\omega_e} + K_d (i_d - \hat{i_d}) \right) dt$$

$$(11) \qquad \widehat{\psi_q} = \int \left(V_q - \hat{i_q} R_s - \widehat{\psi_d} \widehat{\omega_e} + K_q (i_q - \hat{i_q}) \right) dt$$

where K_d, K_q are error gains of the estimated currents $\hat{i_d}, \hat{i_q}$, $\hat{\omega_e}$ denotes the estimated electrical speed and it is obtained by:

$$(12) \qquad \widehat{w_e} = \frac{k_p s + k_i}{s} (\psi_s - \widehat{\psi_s})$$

s is Laplace operator, ψ_s is the inductances $L_{d,q}$ related magnetic flux, and can be expressed using Equations (8), and(9) as:

$$(13) \qquad \psi_s = \sqrt{\psi_d^2 + \psi_q^2}$$

In Equations (10), and (11) the estimated flux linkage expression contains three terms: the conventional voltage-based expressions as stated in Equations (5), and (6); the currents errors multiplied by a proportional gain $K_{d,q}$ for

compensation (the back EMF effect is taken into account as well); and an additive speed related term. The presented flux observer has the ability to withstand the disturbances caused by the iron losses stated in Equations (3), and (4). Thus, the non-measurable torque producing current $i_{dm,qm}$ is therefore estimated indirectly by the proposed flux observer.

As a result, the estimated flux to be introduced into the DTC loop can be stated from Equations (10), and (11) as:

$$(14) \qquad \widehat{\psi}_s = \sqrt{\widehat{\psi_d}^2 + \widehat{\psi_q}^2}$$

The electromagnetic torque used in the DTC algorithm is expressed as a function of the estimated flux in Equations (10), and (11) as:

$$(15) \qquad \widehat{T_e} = \frac{3}{2} P(\widehat{\psi_d} i_q - \widehat{\psi_q} i_d)$$
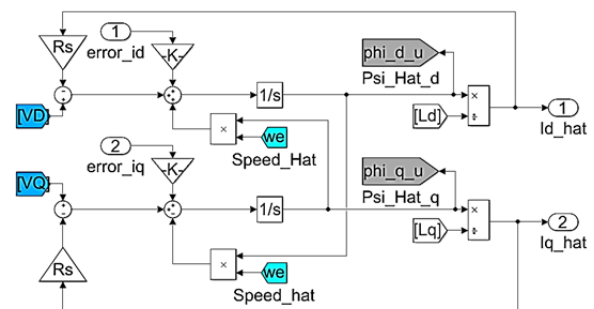

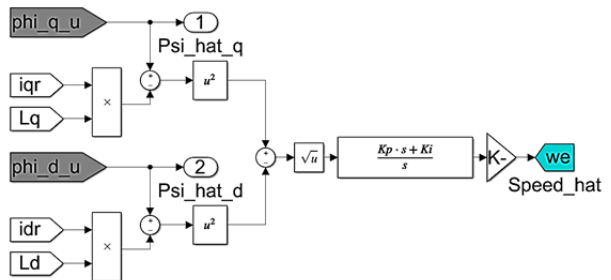Fig.3. MRAS flux observer block diagram in MATLAB/Simulink.

Fig.4. Electrical speed observer block diagram in MATLAB/Simulink.

Fig.3 shows the block diagram of the flux observer, that uses the electrical speed estimator illustrated in Fig.4.

3.3. Modified Flux Angle for DTC Sector Selection

As it is well known, the DTC inner loop requires a 60◦ flux position to precisely generate the appropriate gate pulses signals, according to six predefined sectors. However, in some cases bad flux angle estimation may lead to unstable torque and/or flux response. In conventional flux estimator, the flux angle is mostly affected by miss-tuning of the filters within the voltage-based flux estimator. As a second goal of this paper, a new technique is used to smoothly control the Syn-RM operation. The main idea relies on the use of the rotor angle position θ_r, phase-shifted by an angle δ in Equation (17), which is calculated form Equations (8), and (9) with a speed related offset $K_r \omega_r$ (Fig.5):

$$(16) \qquad \widehat{\theta_f} = 2(\theta_r + \delta + k_r \omega_r)$$

$$(17) \qquad \delta = \arctan(\frac{\psi_q}{\psi_d})$$

Conventional and modified flux angle responses θ_s and $\hat{\theta}_f$, respectively, are illustrated in Fig.6 and Fig.7 for comparison.
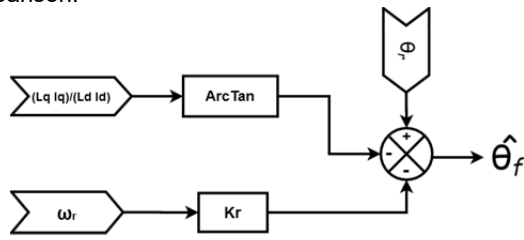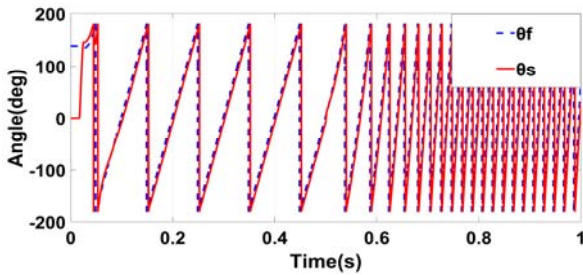

Fig.5. Modified flux angle scheme.

Fig.6. Flux angles used for the DTC algorithm: θ_s conventional angle as in (7); $\hat{\theta}_f$ modified angle as in (16).
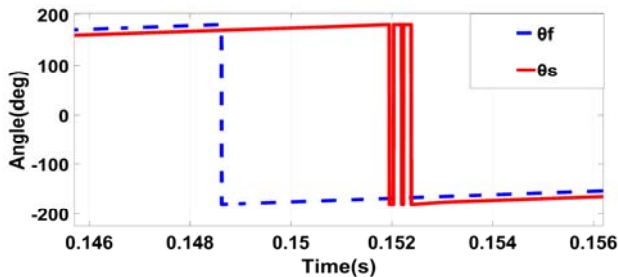

Fig.7. Zoomed-in portion of the flux angles used for the DTC algorithm: θ_s conventional angle as in (7); $\hat{\theta}_f$ modified angle as in (16).

4. Simulation Results and Discussion
4.1. No-Load Test
The control quality and performance of the proposed method are simulated in the MATLAB/Simulink environment, with a Syn-RM motor parameters and inductances *Ld, Lq* are shown in Table 3 and Table 4 in Appendix , step size of 0.005 ms for the Syn-RM model, and of 0.05 ms for the DTC controller and flux observer. The classical DTC is tested using the conventional flux expressed in Equation (13), for a fixed flux reference of 0.9 Wb. A speed controller based on PI is employed, and the torque reference limitation is set to 23 (N.m), the hysteresis bandwidth settings were optimized, as described in subsection 3.1. Torque and flux commands, as well as the selected sector are introduced into a preset switching table, in order to show some performances of the MRAS flux/torque observer. The modified flux angle is utilized with the conventional DTC.
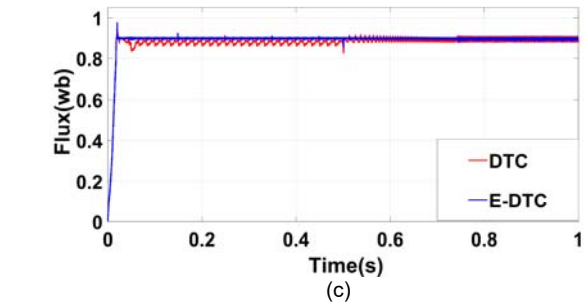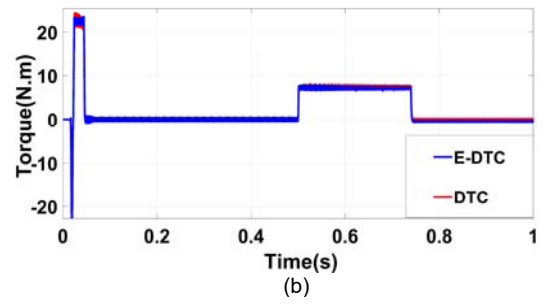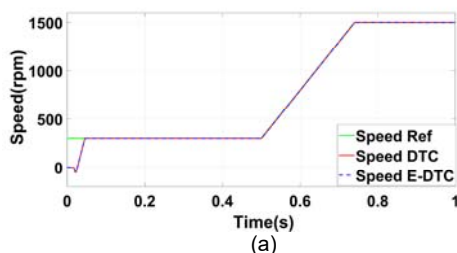

Fig.8. Obtained results using both methods, DTC and E-DTC, for comparison: (a) speed (range 300 - 1500 rpm); (b) electromagnetic torque; (c) magnetic flux.
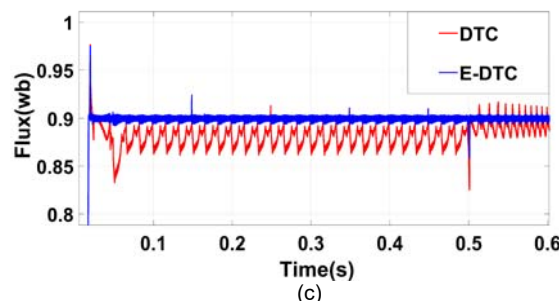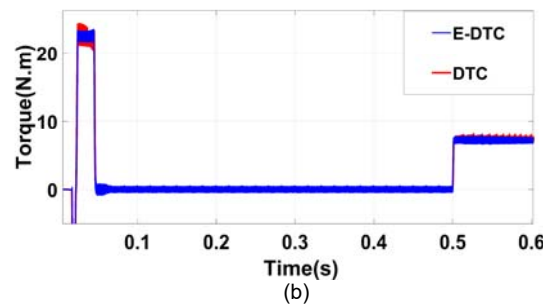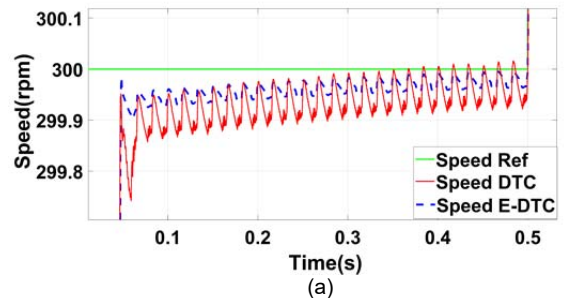

Fig.9. Zoom-in of the obtained results during speed-up at 0.5 s using both methods, DTC and E-DTC, for comparison: (a) speed (b) electromagnetic torque (c) magnetic flux.

The effectiveness of the MRAS flux and torque observer described in Equations (10) and (11) is proved for a wide speed range, starting from stand-still speed up to rated

speed (1500 rpm). Fig.8 presents the no-load test for both DTC an E-DTC.

The speed responses for both techniques are acceptable, as the speed variation is restricted within less than 0.2 rpm band. The torque responses in Fig.8.b and Fig.9.b are remarkable. MRAS observer has reduced the torque ripple magnitude as compared to the conventional DTC results. The flux was smoothly controlled along the simulation period, where its ripple band was significantly reduced from 0.04 Wb to less than 0.001 Wb.

4.2. Full-Load Test

The Syn-RM was fully step loaded (14 N.m) from 0 to 0.02 s. Fig.10 and Fig.11 show the obtained results from 0 to 1500 rpm. As discussed in the no-load test section, the proposed method has a strong effect on the torque ripple reduction, particularly when high torque response is required within the transition state. The flux distortion obtained by using the conventional DTC is almost eliminated, as it is illustrated in Fig.10.c for the low-speed region. The flux response was clearly improved by using the MRAS observer. The electromagnetic torque frequency spectra are shown in Fig.12.a and Fig.12.b for both conventional DTC and E-DTC, respectively. It is obvious that the magnitude of the torque harmonics near to the fundamental frequency, and related to the proposed DTC, were clearly reduced as compared to those of the case of conventional DTC.
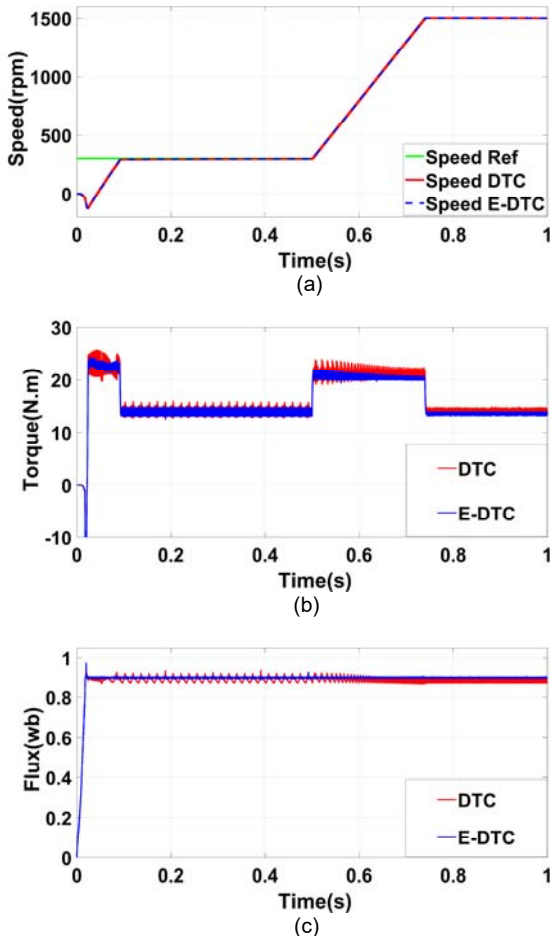

(a)

(b)

(c)

Fig.10. Obtained results using both methods DTC and E-DTC, for comparison: (a) speed (range 300 – 1500 rpm); (b) electromagnetic torque at full load (14 N.m); (c) magnetic flux.
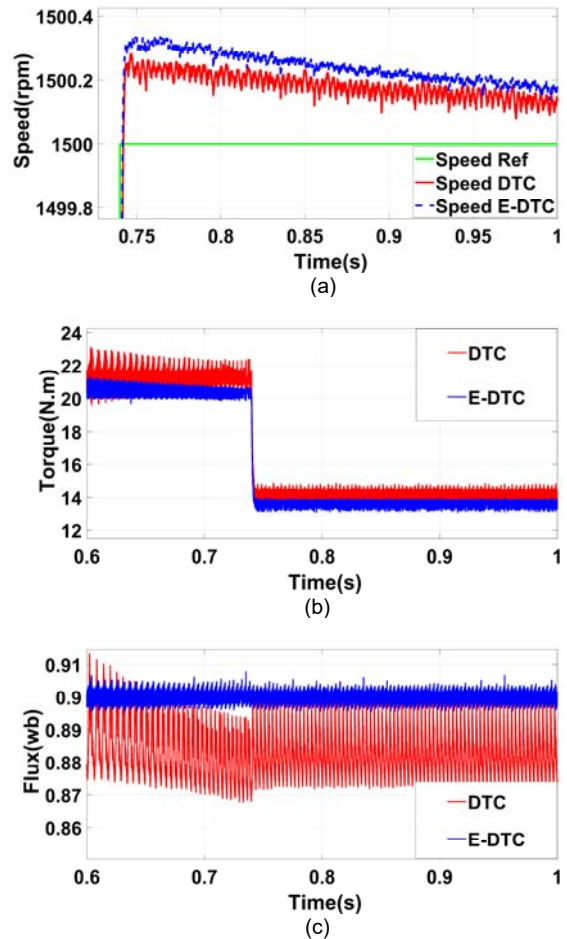

(a)

(b)

(c)

Fig.11. Zoom-in of the obtained results during speed-up at 0.5 s, using both methods DTC and E-DTC, for comparison: (a) speed; (b) electromagnetic torque; (c) magnetic flux.
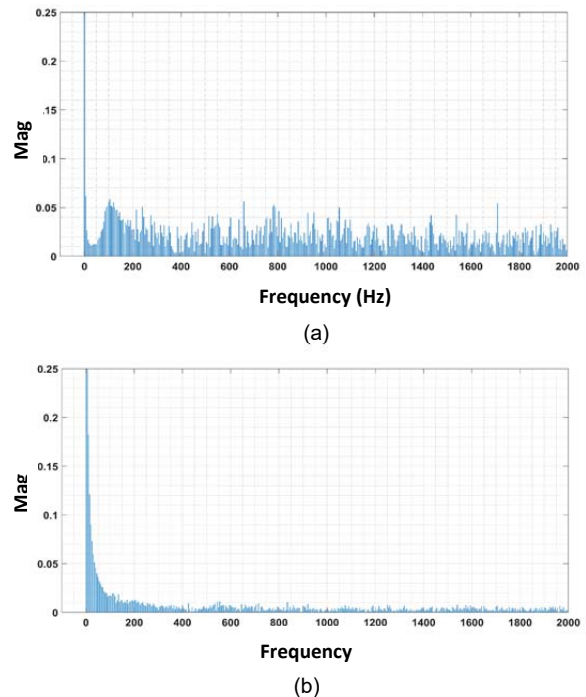

(a)

(b)

Fig.12. Frequency spectra of the electromagnetic torque: (a) conventional DTC; (b) proposed E-DTC.

Table 2. Operational comparison of DTC and E-DTC

		DTC	E-DTC
Average torque ripple	No load test	14.1%	11.0%
	Load test	21.7%	12.1%
Average flux ripple	No load test	3.4%	0.9%
	Load test	3.1%	1.0%

4.3. Modified Flux Angle Test

In order to confirm the robustness of the modified flux-angle estimator described in subsection 3.3, the Syn-RM DTC is tested for both flux-angle estimators. Fig.13 and Fig.14 show the obtained results for torque and flux using conventional flux angle and modified flux angle, respectively. According to the presented results, as high as the speed is increased, the electromagnetic torque and flux are getting high ripple in the case of conventional DTC. However, the torque and flux responses remain stable and smooth for all the speed region, for the case of the proposed E-DTC.
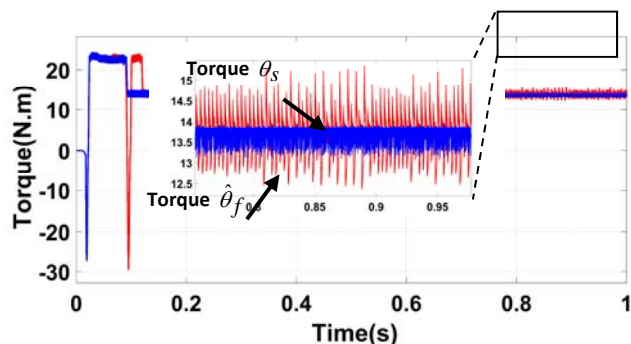

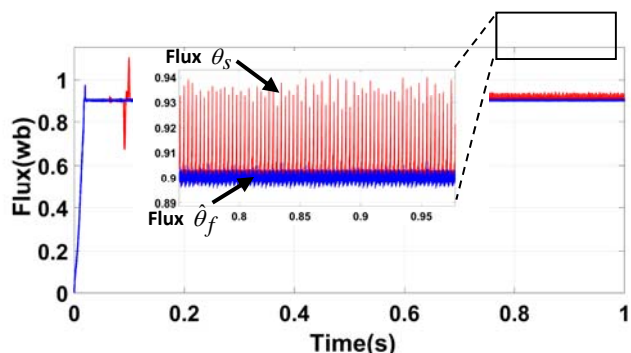Fig.13. Obtained results using both flux-angles estimators: torque θ_s ; torque $\hat{\theta}_f$

Fig.14. Obtained results using both flux-angles estimators: flux θ_s ; flux $\hat{\theta}_f$.

Conclusion

In this paper, a robust DTC was presented using the proposed technique for flux and torque estimation. MRAS model-based observer was employed to estimate the accurate quantities of torque and flux that are required within DTC loop. A new method of flux-angle estimation is presented in this paper, instead of using the conventional voltage-based flux-angle. The performance of the proposed E-DTC is confirmed by simulation. The operational results shown in Table 2 significantly prove the robustness and accuracy of the Syn-RM speed control using the proposed technique.

Appendix

Table 3. Syn-RM model parameters

Rated power	2.2 kw
Rated current	5.7 A
Rated speed	1500 rpm
Rated Torque	14 N.m
N^o of pole pairs	**2**
Moment of inertia (J)	0.0137 Kg
Stator resistance	1.71 Ω

Table 4. *Ld, Lq* Inductances look-up tables used in Syn-RM model

Id(A)	Ld(H)
0,21	0,235
0,39	0,246
0,60	0,251
0,79	0,252
0,99	0,252
1,49	0,249
1,98	0,244
2,51	0,236
3,02	0,225
3,51	0,211
4,03	0,196
4,52	0,182
4,98	0,170
5,45	0,159

Iq(A)	Lq(H)
0,39	0,142
0,62	0,112
0,80	0,098
1,06	0,084
1,52	0,069
1,98	0,061
2,53	0,054
2,98	0,050
3,57	0,046
4,03	0,044
4,55	0,042
5,06	0,041
5,58	0,039
6,09	0,038

Authors:
Mohamed Essalih Boussouar,PHD student, Mohamed Khaider University departement of electrical engineering, Biskra , Algeria , E-mail:m.s.boussouar@gmail.com (Correspondant author)
Khaled Yahia , Prof, Mohamed Khaider University departement of electrical engineering , Biskra , Algeria , E-mail: kd_yahia@yahoo.fr
A.J.M. Cardoso , Prof , University of Beira Interior, Department of Electromechanical Engineering, Covilhã, Portugal E-mail: ajmcardoso@ieee.org
Mohamed Sahraoui, PHD, Mohamed Khaider University departement of electrical engineering, Biskra, Algeria, E-mail: m.sahraoui@univ-biskra.dz

REFERENCES
[1] Yahia, K., Matos, D., Estima, J. O., and Cardoso, A. J. M., Modeling synchronous reluctance motors including saturation, iron losses and mechanical losses, in *International Symposium on Power Electronics, Electrical Drives, Automation and Motion*, Ischia, Italy, pp. 601–606, June 18-20, 2014. https://doi.org/10.1109/SPEEDAM.2014.6871965
[2] Farhan, A., Abdelrahem, M., Hackl, C. M., Kennel, R., Shaltout, A., & Saleh, A., Advanced strategy of speed predictive control for nonlinear synchronous reluctance motors, *Machines*, 8 (3), 44, 2020. https://doi.org/10.3390/machines8030044
[3] Lin, F. J., Chen, S. G., & Hsu, C. W., Intelligent backstepping control of synchronous reluctance motor drive system, *in International Automatic Control Conference*, pp. 1-6, November 2018. https://doi.org/10.1109/CACS.2018.8606767
[4] Lin, F. J., Huang, M. S., Chen, S. G., & Hsu, C. W., Intelligent maximum torque per ampere tracking control of synchronous reluctance motor using recurrent Legendre fuzzy neural network, *IEEE Transactions on Power Electronics*, 34 (12), pp. 12080-12094, 2019. https://doi.org/10.1109/TPEL.2019.2906664
[5] Daryabeigi, E., Zarchi, H. A., Markadeh, G. A., Soltani, J., & Blaabjerg, F., Online MTPA control approach for synchronous reluctance motor drives based on emotional controller, *IEEE Transactions on Power Electronics*, *30* (4), pp. 2157-2166, 2014. https://doi.org/10.1109/TPEL.2014.2323180
[6] De Kock, H. W., & Kamper, M. J.,Dynamic control of the permanent magnet-assisted reluctance synchronous machine, *IET Electric Power Applications*, *1* (2), pp. 153-160, 2007. https://doi.org/10.1049/iet-epa:20060325
[7] Yu, Y., Chang, D., Zheng, X., Mi, Z., Li, X., & Sun, C., Adaptive backstepping based MTPA sensorless control of PM-assisted

SynRM with fully uncertain parameters, *Mathematical Problems in Engineering*, 2018. https://doi.org/10.1155/2018/8405847

[8] N. Bianchi, S. Bolognani, F. Tinazzi and M. Zigliotto, The influence of rotor design on active flux-based sensorless synchronous reluctance motor drives, *2017 IEEE International Symposium on Sensorless Control for Electrical Drives (SLED)*, Catania, Italy, 2017, pp. 7-12, https://doi.org/10.1109/SLED.2017.8078419

[9] Park, J. M., Kim, S. I., Hong, J. P., & Lee, J. H., Rotor design on torque ripple reduction for a synchronous reluctance motor with concentrated winding using response surface methodology, *IEEE Transactions on Magnetics*, *42* (10), pp. 3479-3481, 2006. https://doi.org/10.1109/TMAG.2006.879501

[10] Hesna Aberkane , Djamel Sakri , Djamel Rahem , Enhanced Finite-State Predictive Torque Control of Induction Motor Using Space Vector Modulation , Przegląd Elektrotechniczny ,vol. R. 97, nr 4, pp.41-47,2021 .DOI:10.15199/48.2021.04.07

[11] Lascu, C., Jafarzadeh, S., Fadali, M. S., & Blaabjerg, F., Direct torque control with feedback linearization for induction motor drives, *IEEE Transactions on Power Electronics*, *32* (3), pp. 2072-2080, 2016. https://doi.org/10.1109/TPEL.2016.2564943

[12] Nikzad, M. R., Asaei, B., & Ahmadi, S. O., Discrete duty-cycle-control method for direct torque control of induction motor drives with model predictive solution, *IEEE Transactions on Power Electronics*, *33* (3), pp. 2317-2329, 2017. https://doi.org/10.1109/TPEL.2017.2690304

[13] Mehedi, F., Yahdou, A., Djilali, A. B., & Benbouhenni, H.,Direct torque fuzzy controlled drive for multi-phase IPMSM based on SVM technique, *Journal Européen des Systémes Automatisées*, *53* (2), pp. 259-266, 2020. https://doi.org/10.18280/jesa.530213

[14] Rabi Narayan Mishra & Kanungo Barada Mohanty ,Design and Implementation of a Feedback Linearization Controlled IM Drive via Simplified Neuro-Fuzzy Approach, IETE Journal of Research, 64:2, 209-230,2017 https://doi.org/10.1080/03772063.2017.1351321

[15] M. Siami, D. A. Khaburi and J. Rodríguez, Torque Ripple Reduction of Predictive Torque Control for PMSM Drives With Parameter Mismatch, in *IEEE Transactions on Power Electronics*, vol. 32, no. 9, pp. 7160-7168, Sept. 2017. https://doi.org/10.1109/TPEL.2016.2630274

[16] S. F. Toloue, S. H. Kamali and M. Moallem, Torque Ripple Minimization and Control of a Permanent Magnet Synchronous Motor Using Multiobjective Extremum Seeking, in *IEEE/ASME Transactions on Mechatronics*, vol. 24, no. 5, pp. 2151-2160, Oct. 2019. https://doi.org/10.1109/TMECH.2019.2929390

[17] Hamiti, T., Lubin, T., Baghli, L., & Rezzoug, A.,Modeling of a synchronous reluctance machine accounting for space harmonics in view of torque ripple minimization, *Mathematics and Computers in Simulation*, *81* (2), pp. 354-366, 2020. https://doi.org/10.1016/j.matcom.2010.07.024

[18] Wu, H., Depernet, D., & Lanfranchi, V., Analysis of torque ripple reduction in a segmented-rotor synchronous reluctance machine by optimal currents, *Mathematics and Computers in Simulation*, *158*, pp. 130-147, 2019. https://doi.org/10.1016/j.matcom.2018.07.001

[19] Chen, Q., Yan, Y., Xu, G., Xu, M., & Liu, G.,Principle of torque ripple reduction in synchronous reluctance motors with shifted asymmetrical poles, *IEEE Journal of Emerging and Selected Topics in Power Electronics,* 2019. https://doi.org/10.1109/JESTPE.2019.290970

[20] Xu, M., Liu, G., Zhao, W., & Aamir, N., Minimization of torque ripple in ferrite-assisted synchronous reluctance motors by using asymmetric stator, *AIP Advances*, *8* (5), 056606, 2018. https://doi.org/10.1063/1.5006114

[21] C. Liu, K. Wang, S. Wang, Y. Wang and J. Zhu, Torque ripple reduction of synchronous reluctance machine by using asymmetrical barriers and hybrid magnetic core, in *CES Transactions on Electrical Machines and Systems*, vol. 5, no. 1, pp. 13-20, March 2021. https://doi.org/10.30941/CESTEMS.2021.00003

[22] Yammine, S., Hénaux, C., Fadel, M., & Messine, F., Torque ripple reduction in a SynRM at a constant average torque by means of current harmonics injection, *Progress In Electromagnetics Research*, *80*, pp. 167-180, 2018. http://dx.doi.org/10.2528/PIERC17101801

[23] Bolognani, S., Peretti, L., & Zigliotto, M., Online MTPA control strategy for DTC synchronous-reluctance-motor drives", *IEEE Transactions on Power Electronics*, *26* (1), pp. 20-28, 2010. https://doi.org/10.1109/TPEL.2010.2050493

[24] Zhang, X., Foo, G. H. B., & Rahman, M. F.,"A robust field-weakening approach for direct torque and flux controlled reluctance synchronous motors with extended constant power speed region", *IEEE Transactions on Industrial Electronics*, *67* (3), pp. 1813-1823, 2019. https://doi.org/10.1109/TIE.2019.2903760

[25] H. Wu, D. Depernet, V. Lanfranchi, K. E. K. Benkara and M. A. H. Rasid, "A Novel and Simple Torque Ripple Minimization Method of Synchronous Reluctance Machine Based on Torque Function Method, in *IEEE Transactions on Industrial Electronics*, vol. 68, no. 1, pp. 92-102, Jan. 2021. https://doi.org/10.1109/TIE.2019.2962490

[26] Foo, G. H. B., & Zhang, X.,Robust direct torque control of synchronous reluctance motor drives in the field-weakening region, *IEEE Transactions on Power Electronics*, *32* (2), pp. 1289-1298, 2016. https://doi.org/10.1109/TPEL.2016.2542241

[27] Zarchi, H. A., Arab Markadeh, R., & Soltani, J., Direct torque control of synchronous reluctance motor using feedback linearization including saturation and iron losses, *EPE journal*, *19* (3), pp. 50-62, 2009. https://doi.org/10.1080/09398368.2009.11463725

[28] Boldea, I. Lorand J., Blaabjerg, F, A modified direct torque control (DTC) of reluctance synchronous motor sensorless drive, *Electric Machines & Power Systems*, 28 (2), pp. 115-128, 2000. https://doi.org/10.1080/073135600268405